Journal of Power Sources 189 (2009) 416–422

Contents lists available at ScienceDirect

Journal of Power Sources

journal homepage: www.elsevier.com/locate/jpowsour

Preparation and electrochemical properties of pure lithium cobalt oxide films by electron cyclotron resonance sputtering

Masahiko Hayashi*, Masaya Takahashi, Takahisa Shodai

NTT Energy and Environment Systems Laboratories, Nippon Telegraph and Telephone (NTT) Corporation, Morinosato-Wakamiya 3-1, Atsugi, Kanagawa 243-0198, Japan

ARTICLE INFO

Article history:
Received 11 June 2008
Received in revised form 18 July 2008
Accepted 18 July 2008
Available online 29 July 2008

Keywords:
$LiCoO_2$
ECR sputtering
All-solid-state thin-film lithium battery
Electrode utilization
Raman spectrometry

ABSTRACT

Positive Li–Co–O films for all-solid-state thin-film lithium batteries were prepared by electron cyclotron resonance (ECR) sputtering using Li_xCoO_2 targets (x = 1.0, 1.2, 1.7 and 2.0). The Li–Co–O films prepared using the x = 1.0, 1.2 and 1.7 targets contained a Co_3O_4 impurity phase with high-temperature phase $LiCoO_2$. The film prepared using the x = 2.0 target was found to contain only a pure $LiCoO_2$ phase by Raman spectrometry and the inductively coupled plasma/atomic emission spectrometry (ICP/AES) method, and a thin-film battery using this film exhibited good electrochemical properties as a result of the improved utilization of the positive film.

1. Introduction

Recently electronic devices such as radio frequency (RF) ID tags and paper displays have attracted a lot of attention as portable electronic tools. It is therefore expected that thin and light microbatteries will be developed to reduce the size and weight of these tools. An all-solid-state thin-film lithium battery is a promising microbattery candidate. A thin-film battery has various advantages including no liquid leakage, excellent safety, a long cycle life and a wide operating temperature range [1–8].

Various positive electrode materials have been intensively researched for lithium secondary batteries. In particular, lithium cobalt oxide ($LiCoO_2$) has been widely studied as a positive electrode material owing to its ease of preparation, high voltage, high specific capacity, and long stable cycle life. $LiCoO_2$ thin films are conventionally deposited by using either a dry or a wet process such as the radio frequency magnetron sputtering method [3–6], pulsed laser deposition (PLD) [9–11] and the sol–gel method [12,13].

We previously reported the preparation of $LiCoO_2$ films for thin-film batteries with an electron cyclotron resonance (ECR) sputtering method [8]. Well-crystallized $LiCoO_2$ films were obtained without a post-annealing process when the deposition was undertaken using a high microwave and RF power range in a mixed gas flow with a low O_2 to Ar ratio. Here the microwave power represents the intensity of the ECR plasma and the RF power is applied to a $LiCoO_2$ target to induct the plasma to the target surface. The deposition process, which employs high-energy ionic radiation produced by the ECR sputtering method [14], appears to contribute to the formation of crystallized $LiCoO_2$ film. Moreover, a thin-film battery using the $LiCoO_2$ film showed a high energy density of about 1 mW h cm^{-2} and good cycle performance. However the positive electrode utilization was estimated to be less than 60% from the theoretical capacity per unit volume with respect to $LiCoO_2$: 69 μA h μm^{-1} cm^{-2}. In previous research on the preparation of $LiCoO_2$ films or powders, Co_3O_4 spinel phases that have no electrochemical activity are often produced as impurities because of a deficient Li content [6,8,15]. It is important to increase the Li content in the positive film to obtain the pure $LiCoO_2$ phase. An effective way to achieve this is to optimize the elemental composition of the sputtering target (e.g. the Li/Co ratio in this study).

In this paper, our aim is to prepare positive films consisting of a pure $LiCoO_2$ phase, and to improve the utilization of the positive films. Deposition tests by ECR sputtering were carried out using the Li–Co–O targets with four different Li/Co ratios to increase the Li content of the sputtered film. The crystallographic structures and morphological properties of the sputtered

* Corresponding author. Tel.: +81 46 240 3760; fax: +81 46 270 3721.
E-mail address: mhayashi@aecl.ntt.co.jp (M. Hayashi).

0378-7753/$ – see front matter © 2008 Elsevier B.V. All rights reserved.
doi:10.1016/j.jpowsour.2008.07.050

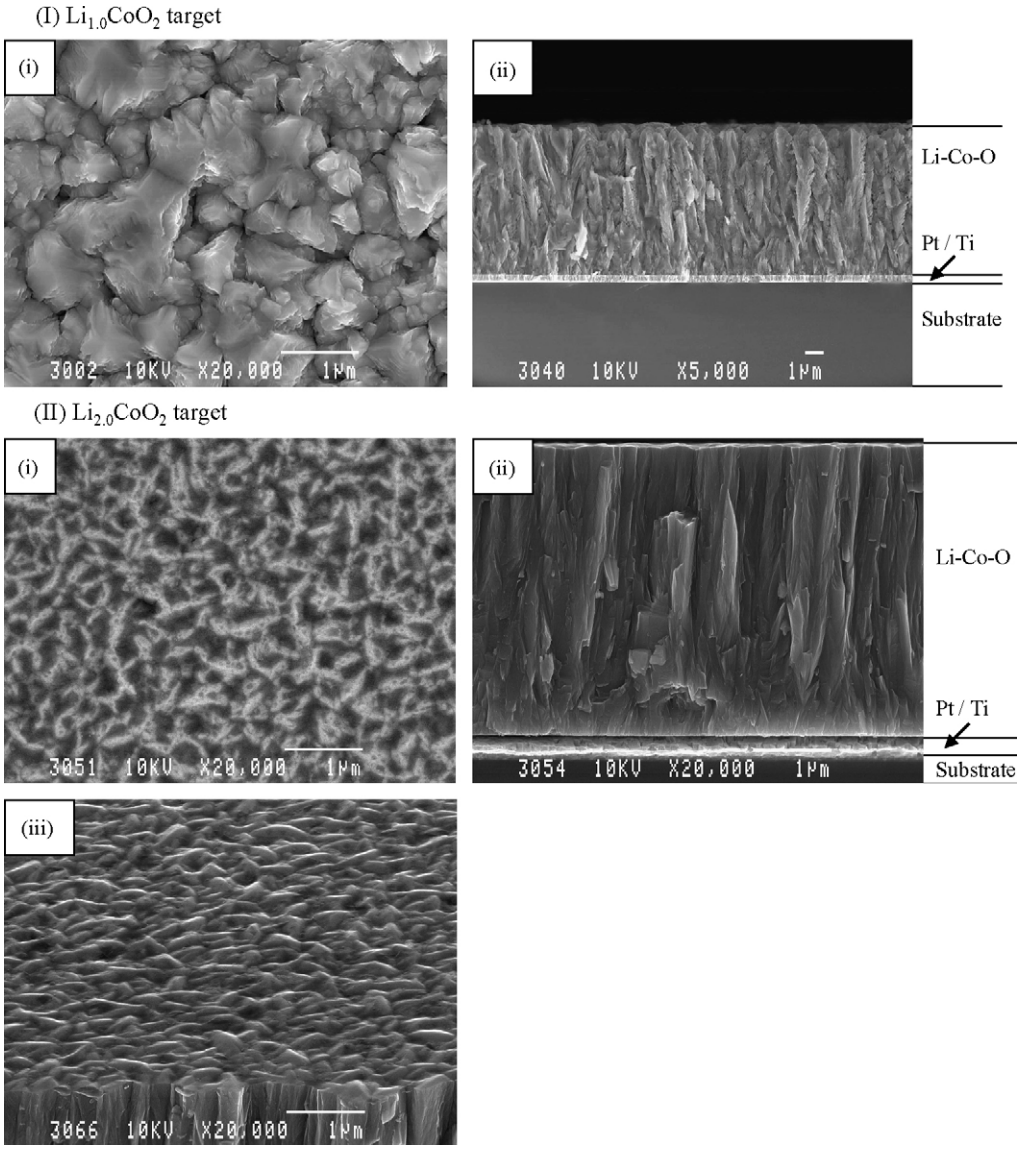

Fig. 1. SEM images of (i) top view, (ii) cross-sectional view and (iii) angled view of Li–Co–O films prepared using (I) $x = 1.0$ and (II) $x = 2.0$ targets. Sputtering time: 6 h.

Li–Co–O films were investigated with various analysis techniques. The most suitable sputtering conditions were determined by estimating the Li content of the sputtered films. Thin-film batteries using the sputtered films as their positive electrodes were investigated in terms of electrochemical performance, and finally the positive film utilization was estimated from the battery properties.

2. Experimental

AFTEX-EC3400 manufactured by MES AFTY Corporation was used as the ECR sputtering equipment as reported elsewhere [8]. In this study, mixtures of $LiCoO_2$ and Li_2CO_3 were used as the sputtering targets. The targets were prepared with Li to Co molar ratios of 1.0, 1.2, 1.7 and 2.0 (x = [Li]/[Co]). These four kinds of the target are denoted as Li_xCoO_2 (x = 1.0, 1.2, 1.7 and 2.0) for the sake of simplicity. The Li–Co–O films were deposited using microwave and RF powers of 800 and 500 W, respectively, under fixed gas ratios of Ar: 20 standard cubic centimeters per minute (sccm) and O_2: 0.5 sccm (total gas pressure: 0.14 Pa). Pt and Ti layers were deposited as current collectors on the quartz glass substrates by RF magnetron sputtering (ANELVA Corp., SPF-430H). The substrates were heated at 300 °C during the deposition process. The morphology of the sputtered films was characterized with a scanning electron microscope (SEM; JEOL Ltd., JSM-890). The oxide films were identified with X-ray diffraction (XRD) analysis equipment (Rigaku Co., Ltd., RINT2100HF). An X-ray with a small incident angle of 5° was used to evaluate the thin oxide film. Raman spectrometry was used to investigate the crystallined phases in the sputtered films. The Li to Co molar ratios (Li/Co) in the films were determined with inductively coupled plasma/atomic emission spectrometry (ICP/AES) equipment (Seiko Instruments Inc., SPS1700). The sample solution for the ICP/AES measurement was prepared by immersing the sputtered Li–Co–O films in hydrochloric acid and nitric acid until the oxide film dissolved completely in the solution.

All-solid-state thin-film lithium batteries composed of the positive Li–Co–O film, a LIPON electrolyte film and a negative Li film were prepared as reported elsewhere [8]. The electrochemical experiments of the resulting thin-film batteries were carried out with a Mac Pile II system (Bio-Logic Science Instruments) in a dry atmosphere at a dew point of less than −50 °C.

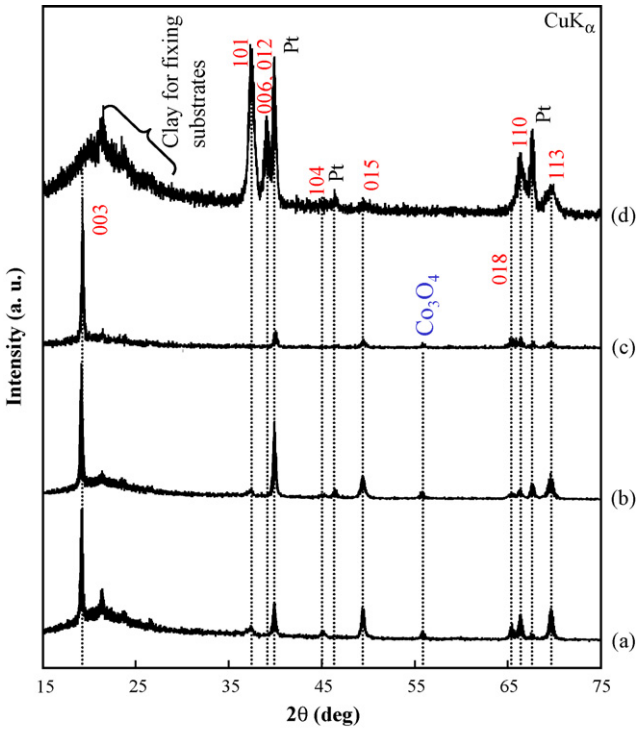

Fig. 2. XRD patterns of Li–Co–O films prepared using targets of (a) $x = 1.0$, (b) $x = 1.2$, (c) $x = 1.7$ and (d) $x = 2.0$ in Li_xCoO_2 targets. Sputtering time: 6 h.

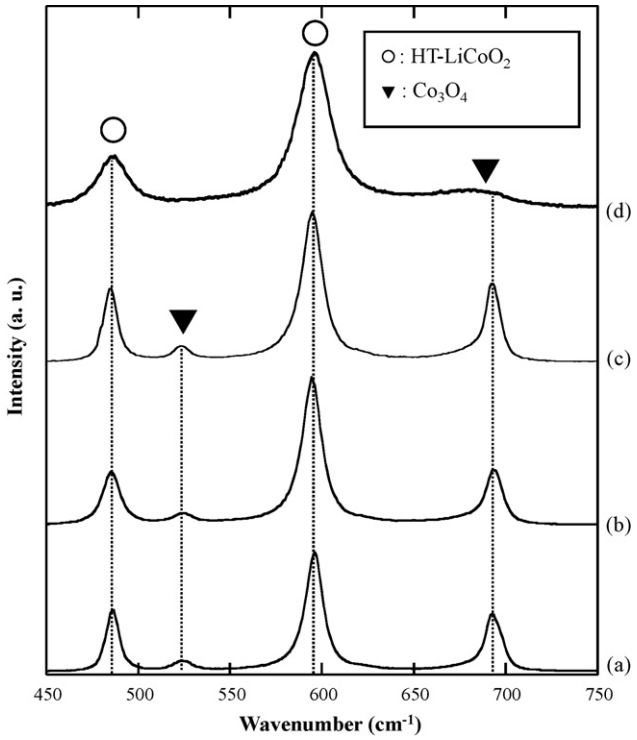

Fig. 3. Raman spectra of Li–Co–O films prepared using targets of (a) $x = 1.0$, (b) $x = 1.2$, (c) $x = 1.7$ and (d) $x = 2.0$ in Li_xCoO_2 targets. Sputtering time: 6 h.

3. Results and discussion

3.1. Characterization of Li–Co–O films prepared using Li_xCoO_2 targets ($x = 1.0$. 1.2, 1.7 and 2.0)

Li–Co–O films were prepared by depositing for 6 h with four different targets where $x = 1.0$, 1.2, 1.7 and 2.0. SEM observation revealed that the morphological structures of the films prepared using the $x = 1.0$, 1.2 and 1.7 targets were largely similar. Fig. 1 shows SEM images of a top view and a cross-sectional view of Li–Co–O films prepared with the $x = 1.0$ and 2.0 targets. Moreover an angled view of the film prepared using $x = 2.0$ is also shown to clarify the surface morphology. As for the film prepared using the $x = 1.0$ target, the surface image revealed that the film surface consisted of submicron grains. The film had a columnar structure as shown in the cross-sectional image. In contrast, the film prepared using the $x = 2.0$ target had a smoother and more homogeneous surface without the large prominent grains from the surface and the angled images seen in Fig. 1(II). As shown in the cross-sectional images, the film prepared with the $x = 2.0$ target also had a fine columnar structure which consisted of smaller grains than those of the film prepared with the $x = 1.0$ target. The oxide films obtained in this study are composed of polycrystalline grains. A large number of grain boundaries connect the oxide crystallites to each other in the films. The grain boundaries may act as barriers when Li ions diffuse in the oxide films. In a film with a columnar structure, the electrode performance, especially with high-rate charging and discharging, would be improved by reducing the number of grain boundaries. It is therefore important to investigate the electrochemical properties of the Li–Co–O film, prepared using the $x = 2.0$ target, with a finer columnar structure. The cross-sectional images showed that the sputtered Li–Co–O films prepared using the $x = 1.0$, 1.2, 1.7 and 2.0 targets were found to be 7.1, 6.9, 6.9 and 3.7 μm thick, respectively.

Fig. 2 shows XRD patterns of Li–Co–O films prepared using the $x = 1.0$. 1.2 1.7 and 2.0 targets under the same sputtering condition. Miller indices corresponding to $LiCoO_2$ (JCPDS No. 50-0653) and the peak positions of Co_3O_4 (No. 43-1003) and Pt are indicated in this figure. It is well known that Co_3O_4 coexists with $LiCoO_2$ because of the deficiency in the Li content of films prepared by the sputtering method [3–5,8]. Small peaks near 56° identified as Co_3O_4 are observed in all the patterns except for $x = 2.0$. However, it is difficult to discuss this quantitatively for oxide films with a crystal orientation, and it is suggested that the main phase of these films is $LiCoO_2$, which also contain a small amount of Co_3O_4. Moreover these films have sharp and strong peaks of (0 0 3), indicating the high degree of oxide crystallization. On the other hand, the pattern of the film prepared using the $x = 2.0$ target was clearly different from the patterns of the other films. All the peaks, excluding Pt and clays for fixing substrates, of the film using $x = 2.0$ was identified as $LiCoO_2$, and the main peak was not (0 0 3) but (1 0 1). The degree of oxide crystallization is rather low compared with that of the other films. This behavior suggests that the growth mechanism of the oxide films changes greatly between $x = 1.7$ and 2.0.

Raman spectroscopic analysis was carried out to investigate the oxide phase in the Li–Co–O films. It is well known that a high-temperature phase (HT-$LiCoO_2$), a low-temperature phase (LT-$LiCoO_2$), and a Co_3O_4 spinel phase can be produced in the sputtered Li–Co–O films [6,15,16]. Of these three phases, HT-$LiCoO_2$ ($R\bar{3}m$) exhibits excellent electrochemical properties as the cathode material in lithium secondary batteries. Raman spectrometry is a useful technique for investigating which phases are contained in sputtered Li–Co–O films [6,15,16]. Fig. 3 shows Raman spectra of Li–Co–O films prepared using $x = 1.0$, 1.2, 1.7, and 2.0 targets. Two peaks at 485 and 595 cm^{-1} corresponding to HT-$LiCoO_2$ are observed in all the films. This indicates that HT-$LiCoO_2$ can be prepared without a post-annealing process under the sputtering conditions used in this study. On the other hand, no peaks corre-

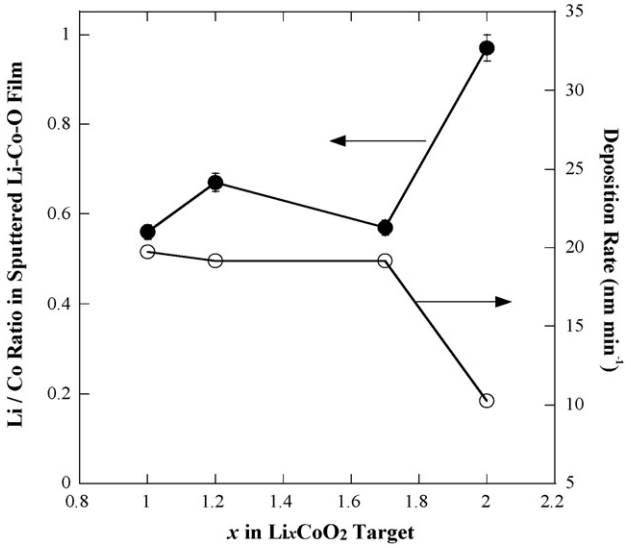

Fig. 4. Dependence of Li/Co ratios in sputtered Li–Co–O films and deposition rates on x in Li_xCoO_2 targets.

sponding to the LT-$LiCoO_2$ phase with a spinel structure ($Fd3m$) were observed in any of all the films at 445, 478, 583 or 603 cm^{-1} [16]. In the films other than the $x = 2.0$ film, two peaks at 520 and 690 cm^{-1} were also observed corresponding to the Co_3O_4 phase. In the $x = 2.0$ film, a rather broad peak was observed at 690 cm^{-1}, which indicated that a very small amount of Co_3O_4 phase was present in this film. Additionally the peaks of the $x = 2.0$ film are broad compared with those of the other films. This is due to the low degree of oxide crystallization. This trend in the spectrum is consistent with the XRD pattern results shown in Fig. 2. Here Raman spectrometry is unsuitable for quantitative discussions of, for example, the content of the impurity phase, and it is necessary to investigate the Li/Co ratios in the sputtered films by using a quantitative analysis technique such as the ICP/AES method.

The molar ratios of Li and Co (Li/Co) contained in the Li–Co–O films were quantitatively evaluated with the ICP/AES method. Fig. 4 shows the dependence of the Li/Co ratios on x in the Li_xCoO_2 targets, together with the deposition rates which were calculated from the cross-sectional SEM images. The deposition rates had almost the same value of about 18 nm min^{-1} between $x = 1.0$ and 1.7, and the rate for the $x = 2.0$ target decreased greatly to 10 nm min^{-1}. The films other than the $x = 2.0$ film showed Li/Co ratios of about 60%. This value suggests that the films contained not only $LiCoO_2$ phases but also about 40% of Co_3O_4 phases. On the other hand, the Li/Co ratio of the film prepared using the $x = 2.0$ target was almost 1.0, which indicated that the oxide film was composed of pure $LiCoO_2$ phase. This is consistent with the results obtained by XRD measurement and Raman spectrometry shown in Figs. 2 and 3, respectively. When preparing the Li–Co–O films, it appears that the Co_3O_4 phase is produced owing to a deficiency in the Li species which can bounce off the target and reach the substrate surface. This deficiency may be caused by the low sputtering yield on Li contained in the Li_xCoO_2 targets. In this study, the Li_xCoO_2 targets are composed of $LiCoO_2$ and Li_2CO_3. These two compounds have intrinsic sputtering yields. When using the $x = 2.0$ target, the great change in the Li/Co ratios might be caused by the mixed state of $LiCoO_2$ and Li_2CO_3 in the targets. For example, when one compound with a higher yield was entirely covered with the other compound with a lower yield, a large amount of Li species might bounce out form the target and reach the substrate surface. And consequently a pure $LiCoO_2$ phase might be obtained when using the $x = 2.0$ target.

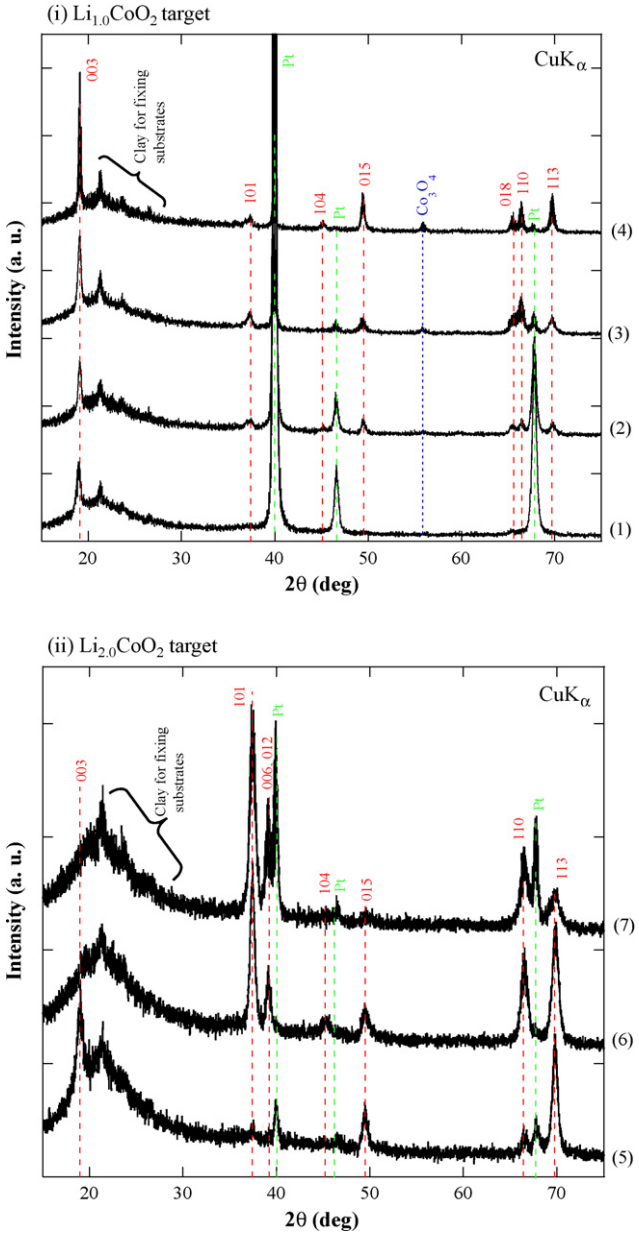

Fig. 5. XRD patterns of Li–Co–O films with various film thicknesses prepared using (i) $x = 1.0$ and (ii) $x = 2.0$ targets. Film thickness: (1) 0.13 μm, (2) 0.53 μm, (3) 2.3 μm, (4) 7.1 μm, (5) 0.70 μm, (6) 2.1 μm, and (7) 3.7 μm.

Considering the large change in the deposition rate at $x = 2.0$, the deposition process using the $x = 2.0$ target appears to proceed via another reaction mechanism when using the other targets as described above. As a result, such a slow deposition rate at $x = 2.0$ may be a disadvantage as regards the battery manufacturing cost, however the Li–Co–O film containing no impurity phases that was prepared using the $x = 2.0$ target is expected to exhibit good electrochemical properties with high positive electrode utilization.

3.2. Characterization of Li–Co–O films with various thicknesses using Li_xCoO_2 targets ($x = 1.0$, 1.2, 1.7, and 2.0)

Fig. 5 shows XRD patterns of Li–Co–O films with various thicknesses prepared using $Li_{1.0}CoO_2$ and $Li_{2.0}CoO_2$ targets. All the patterns of the films prepared using the $x = 1.0$ target have char-

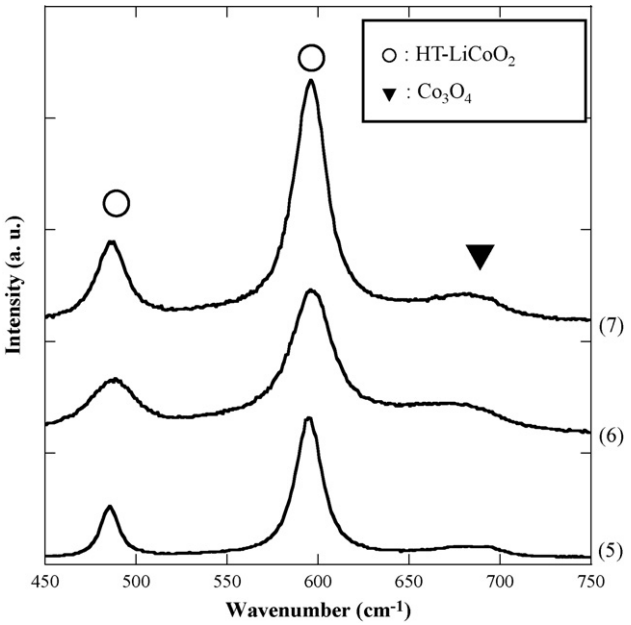

Fig. 6. Raman spectra of Li–Co–O films prepared using the $Li_{2.0}CoO_2$ target with thicknesses of (5) 0.70 μm, (6) 2.1 μm, and (7) 3.7 μm.

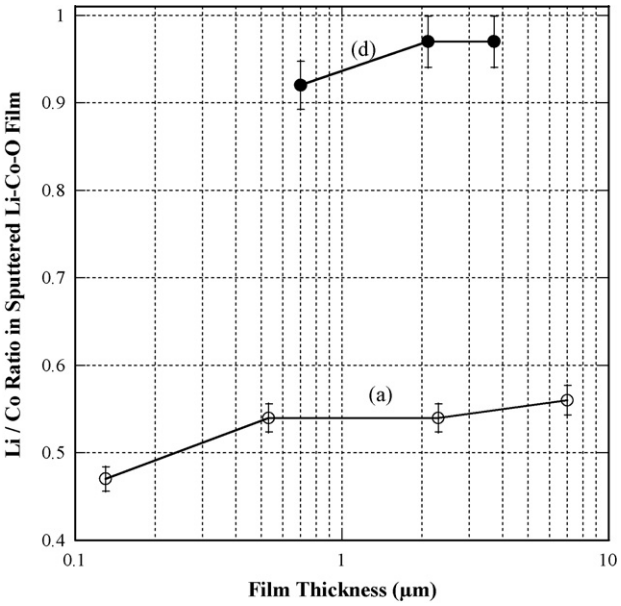

Fig. 7. Dependences of Li/Co ratios in sputtered Li–Co–O films prepared using (a) $Li_{1.0}CoO_2$ and (d) $Li_{2.0}CoO_2$ targets on the film thickness.

acteristic peaks of (0 0 3) near 19°, although there are also small peaks at 56° that correspond to Co_3O_4 phases. These tendencies are similar to those shown in Fig. 2(a). All the peaks corresponding to $LiCoO_2$ phases become stronger and sharper as the film thickness increases. There were no significant differences in the peak positions of any of the films. This suggests that the oxide crystals grow monotonously in the same way despite the increasing film thickness. Such behavior was almost the same for the films prepared using the $x = 1.2$ and 1.7 targets. This result is clearly different from that obtained using the $x = 2.0$ target as described below. Compared with the $x = 1.0$ films, the films prepared using the $x = 2.0$ exhibit a lower degree of crystallization without containing Co_3O_4 impurity phases. Moreover, the peaks in the XRD patterns change with increasing the film thickness. The 0.70-μm thick film has strong peaks of (0 0 3) and (1 1 3) and small peaks of (1 0 1), (0 1 5) and (1 1 0). On the other hand, the (0 0 3) peak completely disappears in XRD patterns of the films with thicknesses of 2.1 and 3.7 μm. By contrast, these films have main peaks of (1 0 1) and sharp peaks of (0 0 6), (0 1 2) and (1 1 0). Among these peaks, (0 0 6) and (0 1 2) are not observed at all in the 0.70 μm thick film. It was clear that the crystal growth mechanism of the Li–Co–O film varied depending on the film thickness when prepared using the $x = 2.0$ target. According to previous reports by Bates et al. [3,4], when preparing $LiCoO_2$ films by RF magnetron sputtering, (1 0 1) and (1 0 4) peaks were clearly observed, and the (0 0 3) plane was not observed for films thicker than about 1 μm. When using the $x = 1.0$ target, these results are different from ours where the XRD pattern of the film has a strong and sharp (0 0 3) peak, independent of film thickness. On the other hand, when using the $x = 2.0$ target, the results of this study, namely that the (0 0 3) peaks are not observed in films more than 2.1-μm thick, are very similar to those reported by Bates et al. This suggests that the growth of the sputtered Li–Co–O film is affected by the ratios of the Li and Co contained in the sputtering targets.

Fig. 6 shows Raman spectra of Li–Co–O films with various thicknesses prepared using the $Li_{2.0}CoO_2$ targets. With all the films, two peaks at 485 and 595 cm^{-1} were observed corresponding to HT-$LiCoO_2$, however the peak at 690 cm^{-1} corresponding to Co_3O_4 was very small and broad. This result revealed that all Li–Co–O films prepared using the $x = 2.0$ target were composed of pure HT-$LiCoO_2$ phase, regardless of the film thickness. In addition, the Raman spectra of these films are not affected by changes in crystal orientation caused by the film thickness shown in Fig. 5(II).

Fig. 7 shows the film thickness dependence of the Li/Co ratios in sputtered Li–Co–O films prepared using $x = 1.0$ and 2.0 targets. The Li/Co ratios of the Li–Co–O films prepared using the $x = 1.0$ targets have values in the 0.47 and 0.57 range. This result shown in Fig. 7(a) is almost the same as that for the films using $x = 1.2$ and 1.7 targets. These Li/Co ratios of less than 1.0 indicate that the films contain the Co_3O_4 impurity phase, as shown in Fig. 3, due to Li deficiency. On the other hand, the Li/Co ratios of the films using the $x = 2.0$ target increased greatly to values of more than 0.9 as shown in Fig. 7(d). In particular, films with thicknesses of 2.1 and 3.7 μm exhibit Li/Co ratios of almost 1.0. On the basis of these results obtained by ICP/AES method and Raman spectrometry, it was found that the Li–Co–O films obtained using the $x = 2.0$ target were composed of pure $LiCoO_2$ phase. These results suggest that pure $LiCoO_2$ films prepared using the $x = 2.0$ target would improve the utilization of the positive electrode and provide larger discharge capacities per unit volume of film. An interesting feature of all the films was that the Li/Co ratios increased with increasing film thickness. This finding indicates that Li species that bounce from the target may react with the Pt/Ti layer on the substrates during the sputtering process. This behavior will be discussed in detail in a forthcoming paper.

As described above, the crystallographic structure and orientation, the film composition such as the Li/Co ratio, and the oxide phases such as $LiCoO_2$ and Co_3O_4 with respect to the Li–Co–O films obtained when using the $x = 1.0$, 1.2, and 1.7 targets were very different when using the $x = 2.0$ targets. Based on the finding that pure $LiCoO_2$ phase with characteristic crystallographic features was obtained with the $x = 2.0$ target, the film deposition may be affected by the Li/Co ratios in the deposition process where Li, Co and O species bounce out from the Li_xCoO_2 targets and strike the substrate surface. The film deposition using the $x = 2.0$ target may be also affected by the mixed state and the differences in the sputtering yields of $LiCoO_2$ and Li_2CO_3 contained in the targets as stated in Section 3.2.

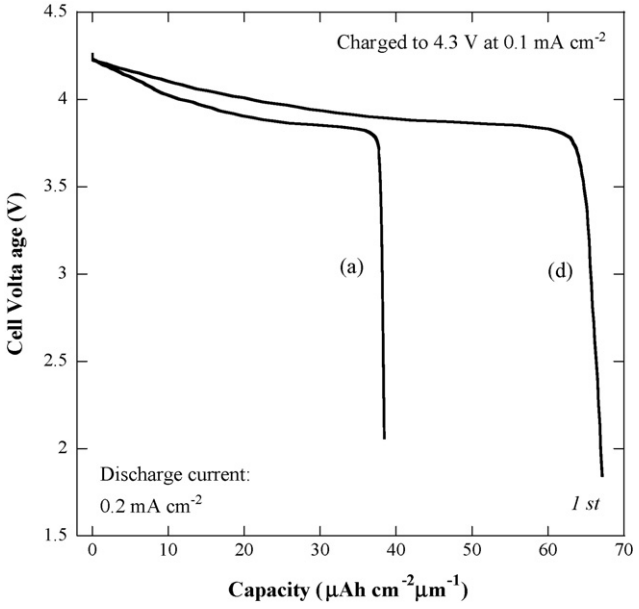

Fig. 8. Discharge curves of all-solid-state thin-film lithium batteries using positive Li–Co–O films prepared with (a) $Li_{1.0}CoO_2$ and (d) $Li_{2.0}CoO_2$ targets. Sputtering time: 6 h. Film thickness: (a) 7.1 μm and (d) 3.7 μm.

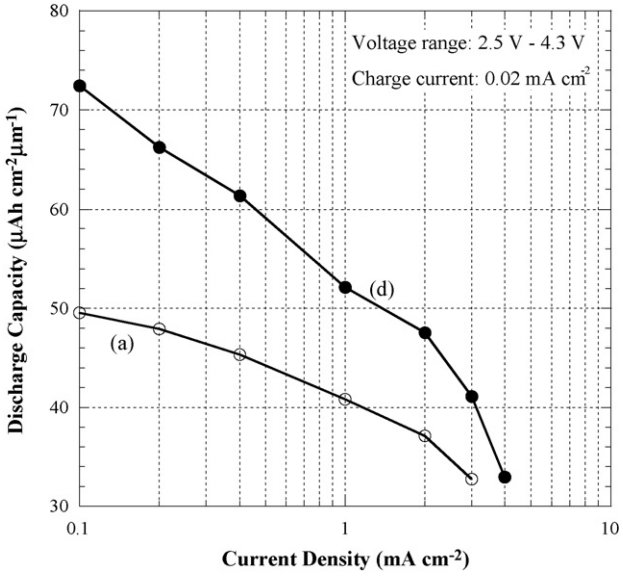

Fig. 9. Discharge rate properties of all-solid-state thin-film lithium batteries using positive Li–Co–O films prepared with (a) $Li_{1.0}CoO_2$ and (d) $Li_{2.0}CoO_2$ targets. Sputtering time: 6 h. Film thickness: (a) 7.1 μm and (d) 3.7 μm.

3.3. *Electrochemical properties of Li–Co–O films prepared using $Li_{1.0}CoO_2$ and $Li_{2.0}CoO_2$ targets*

Fig. 8 shows discharge curves of all-solid-state thin-film lithium batteries using positive Li–Co–O films (sputtering time: 6 h) prepared with $Li_{1.0}CoO_2$ and $Li_{2.0}CoO_2$ targets under a galvanostatic condition of 0.2 mA cm^{-2}. In this figure, the discharge capacities are normalized by the unit volume of the Li–Co–O film to evaluate the utilization of the positive electrode. When the discharge capacities are evaluated in terms of the effective area of the battery, both batteries exhibit almost the same energy densities of about 1 mW h cm^{-2} even though the two positive electrodes have different film thicknesses. However, there was clearly a large difference in capacities per unit volume as shown in this figure. Thin-film batteries using the positive Li–Co–O films prepared with the $x = 1.0$ and 2.0 targets exhibited the discharge capacities of 38 and 67 μA h cm^{-2} $μm^{-1}$, respectively. It is considered that the differences in these capacities reflect the amount of impurity phase in the positive films. Electrode utilization, which is calculated in terms of the discharge capacities shown in Fig. 8, of positive Li–Co–O films prepared with $x = 1.0$ and 2.0 targets is shown in Table 1, together with the Li/Co ratios of the films used in the discharge tests shown in Fig. 7. From this table, the positive film prepared with the $x = 2.0$ target exhibited higher utilization than that prepared with the $x = 1.0$ target. It should be noted that the film for the $x = 2.0$ target exhibited almost 100% utilization. Furthermore the utilization for the $x = 1.0$ and 2.0 targets is consistent with the Li/Co ratios in the films. As a result, a high utilization for the $x = 2.0$ target found to be achieved by reducing the content of the Co_3O_4 impurity phase in the film.

Table 1
Utilization and Li/Co ratios of positive Li–Co–O films prepared with (a) $Li_{1.0}CoO_2$ and (d) $Li_{2.0}CoO_2$ targets (sputtering time: 6 h) incorporated in all-solid-state thin-film lithium batteries

Target	Positive film utilization (%)	Li/Co[a] (molar ratio)
$Li_{1.0}CoO_2$	55	0.56
$Li_{2.0}CoO_2$	97	0.97

[a] Measured by ICP/AES method (Fig. 7).

Fig. 9 shows discharge capacities of all-solid-state thin-film lithium batteries using Li–Co–O films prepared with $Li_{1.0}CoO_2$ and $Li_{2.0}CoO_2$ targets under a galvanostatic condition with various current densities. The battery using the Li–Co–O film prepared using the $x = 2.0$ target had a larger capacity than the $x = 1.0$ target over the entire current range. This is because of higher utilization and lower resistance of the positive film prepared using the $x = 2.0$ target in the battery. The electrical resistance of both films should have obvious differences since the positive film using the $x = 1.0$ target is almost twice as thick as the film using the $x = 2.0$ target. This reduced thickness of the film using the $x = 2.0$ target appears to improve the discharge rate performances by reducing the diffusion length of the Li ions in the film. The batteries can also be discharged under the conditions of mA order. These high performances would meet the demand for high-power thin-film lithium batteries.

4. Conclusions

Positive Li–Co–O films for thin-film lithium batteries were prepared by ECR sputtering using Li_xCoO_2 targets ($x = 1.0$, 1.2, 1.7 and 2.0). Li–Co–O films prepared using $x = 1.0$, 1.2, and 1.7 contained Co_3O_4 impurity phases with HT-$LiCoO_2$ phases. The XRD patterns of these films revealed that they exhibited a high degree of oxide crystallization with sharp and strong (0 0 3) peaks, regardless of the film thickness. On the other hand, the film prepared using the $x = 2.0$ target contained only the pure $LiCoO_2$ phase. Compared with the other targets, the crystal structure of the film obtained using the $x = 2.0$ target changed with increasing the film thickness. As mentioned above, the crystallographic and compositional properties changed greatly depending on the Li_xCoO_2 target used. Thin-film lithium batteries containing $LiCoO_2$ films prepared using the $x = 2.0$ target provided higher energy densities of about 1 mW h cm^{-2} and higher utilization of the positive films, compared with the other targets, as the positive films contained no Co_3O_4 impurity phases. Moreover the thin-film batteries could be discharged even at high current densities of mA order. It was found that the battery performances could be improved by using positive $LiCoO_2$ films prepared with appropriate sputtering targets.

Acknowledgements

We express our gratitude to Mr. Kosuke Katsura and Dr. Tadahito Aoki of NTT Energy and Environment Systems Laboratories for their continuous guidance and encouragement during the course of this study. We also thank Mr. Shoji Oriuchi of NTT Facilities Research Institute Inc. for his assistance in the experiments.

References

[1] J. Yamaki, H. Ohtsuka, T. Shodai, Solid State Ionics 86–88 (1996) 1279.
[2] H. Ohtsuka, Y. Sakurai, Solid State Ionics 144 (2001) 59.
[3] J.B. Bates, N.J. Dudney, B.J. Neudecker, F.X. Hart, H.P. Jun, S.A. Hackney, J. Electrochem. Soc. 147 (2000) 59.
[4] J.B. Bates, N.J. Dudney, B. Neudecker, A. Ueda, C.D. Evans, Solid State Ionics 135 (2000) 33.
[5] J.F. Whitacre, W.C. West, E. Brandon, B.V. Ratnakumar, J. Electrochem. Soc. 148 (2001) A1078.
[6] C.-L. Liao, K.-Z. Fung, J. Power Sources 128 (2004) 263.
[7] J. Schwenzel, V. Thangadurai, W. Weppner, J. Power Sources 154 (2006) 232.
[8] M. Hayashi, M. Takahashi, Y. Sakurai, J. Power Sources 174 (2007) 990.
[9] H. Xia, L. Lu, G. Ceder, J. Power Sources 159 (2006) 1422.
[10] Y. Iriyama, M. Inaba, T. Abe, Z. Ogumi, J. Power Sources 94 (2001) 175.
[11] Y. Iriyama, H. Kurita, I. Yamada, T. Abe, Z. Ogumi, J. Power Sources 137 (2004) 111.
[12] Y.H. Rho, K. Kanamura, T. Umegaki, J. Electrochem. Soc. 150 (2003) A107.
[13] M. Kim, K. Park, D. Kim, J. Son, H. Kim, J. Kor. Ceram. Soc. 38 (2001) 777.
[14] S. Hirono, S. Umemura, M. Tomita, R. Kaneko, Appl. Phys. Lett. 80 (2002) 425.
[15] W. Huang, R. Frech, Solid State Ionics 86 (1996) 395.
[16] L. Mendoza, R. Baddour-Hadjean, M. Cassir, J.P. Pereira-Ramos, Appl. Surf. Sci. 225 (2004) 356.